

Title: Wnt, Ptk7, and FGFR1 expression gradients control trunk positional identity in planarian regeneration

Authors and Affiliations:

Rachel Lander¹

Christian P. Petersen^{*1,2}

1-Department of Molecular Biosciences, Northwestern University, Evanston, IL 60208

2-Robert Lurie Comprehensive Cancer Center, Northwestern University, Evanston IL 60208

*-corresponding author, christian-p-petersen@northwestern.edu

Competing interests statement:

The authors declare no competing interests

Abstract

Mechanisms enabling positional identity re-establishment are likely critical for tissue regeneration. Planarians use Wnt/beta-catenin signaling to polarize the termini of their anteroposterior axis, but little is known about how regeneration signaling restores regionalization along body or organ axes. We identify three genes expressed constitutively in overlapping body-wide transcriptional gradients that control trunk-tail positional identity in regeneration. *ptk7* encodes a trunk-expressed kinase-dead Wnt co-receptor, *wntP-2* encodes a posterior-expressed Wnt ligand, and *ndl-3* encodes an anterior-expressed homolog of conserved FGFR1/*nou-darake* decoy receptors. *ptk7* and *wntP-2* maintain and allow appropriate regeneration of trunk tissue position independently of canonical Wnt signaling and with suppression of *ndl-3* expression in the posterior. These results suggest that restoration of regional identity in regeneration involves the interpretation and re-establishment of axis-wide transcriptional gradients of signaling molecules.

Introduction

Robust pattern control is a central but poorly understood feature of regenerative abilities (Wolpert 1969; French et al. 1976). Animals cannot anticipate how a given injury will alter tissue composition, so regeneration likely depends critically on the re-establishment of missing tissue identity. Planarians use pluripotent stem cells to regenerate from nearly any amputation to restore a complete set of regionalized tissues, including cephalic ganglia in the anterior and a pharynx and mouth in the trunk, and are a model of positional restoration after amputation (Reddien 2011; Adler and Sánchez Alvarado 2015). Canonical Wnt signaling controls anterior-versus-posterior pole identity in planarian regeneration, with principal upstream determinants *wnt1* expressed at the posterior pole (Petersen and Reddien 2009; Gurley et al. 2010) and the secreted Wnt inhibitor *notum* expressed at the anterior pole (Petersen and Reddien 2011), both activated transcriptionally early after wounding. Inhibition of Wnt signaling components β -*catenin-1*, *wnt1*, *Evi/wntless*, *Dvl-1/2* and *teashirt* causes regeneration of ectopic heads (Gurley et al. 2008; Iglesias et al. 2008; Petersen and Reddien 2008; Petersen and Reddien 2009; Owen et al. 2015; Reuter et al. 2015); conversely, inhibition of *APC* or *notum* can cause regeneration of ectopic tails (Gurley et al. 2008; Petersen and Reddien 2011). Other pathways participate in head or tail regeneration, with Hedgehog signaling influencing injury-induced *wnt1* expression (Rink et al. 2009), several transcription factors required for head formation (*prep*, *foxD*, *zic-1/zicA*, *pbx*, *egr-4*) (Felix and Aboobaker 2010; Blassberg et al. 2013; Chen et al. 2013; Fraguas et al. 2014; Scimone et al. 2014; Vásquez-Doorman and Petersen 2014; Vogg et al. 2014) and/or tail formation (*junli-1*, *pitx*, *pbx*) (Blassberg et al. 2013; Chen et al. 2013; Currie and Pearson 2013; Marz et al. 2013; Tejada-Romero et al. 2015), and influenced by gap junction and calcium signaling (Oviedo et al. 2010; Zhang et al. 2011). However, comparatively little is known about the restoration of positional information along the head-to-tail body axis through regeneration. Expression profiling and homology searching have identified a cohort of factors related to Wnt, Hox, and FGF signaling expressed regionally in domains along the anteroposterior (A-P) axis in planarians (Cebrià et al. 2002; Petersen and Reddien 2008; Reddien 2011; Owen et al. 2015; Reuter et al. 2015). These factors could in principle form a molecular coordinate system that re-specifies axis identity in regeneration and have been termed “positional control genes” (PCGs) (Witchley et al. 2013). However, few phenotypes of positional displacement have been reported

from perturbation of PCGs (Cebrià et al. 2002; Kobayashi et al. 2007), so it remains unclear how the majority of these genes participate in regeneration.

Results

To uncover programs responsible for patterning along the body axis, we examined PCGs as defined by prior homology and expression profiling studies (Petersen and Reddien 2008; Reddien 2011; Witchley et al. 2013; Owen et al. 2015; Reuter et al. 2015) and found a unique expression pattern for a planarian homolog of *ptk7*, expressed in an animal-wide graded fashion maximally in the trunk, and also the CNS and pharynx (Figure 1A, Figure 1-figure supplement 1). Ptk7 proteins encode cell-surface Wnt co-receptors with a predicted intracellular pseudokinase domain that participate in noncanonical, β -catenin-independent Wnt signaling (Lu et al. 2004), and can either weakly suppress or activate canonical β -catenin-dependent Wnt signaling in a context-dependent manner (Peradziryi et al. 2011; Puppo et al. 2011; Hayes et al. 2013; Bin-Nun et al. 2014). Like other described PCGs, planarian *ptk7* was expressed in *collagen*⁺ cells of the body-wall musculature (Witchley et al. 2013) and aspects of its expression domain could become re-established after amputation even in irradiated animals lacking neoblasts and the ability to form new tissues (Figure 1A-C). In *ptk7(RNAi)* animals amputated to remove both head and tail, regeneration produced a normal head and tail (35/35) but caused formation of an ectopic posterior mouth at a high penetrance (83%, n=35) and, more rarely, formation of an ectopic posterior pharynx with broadly normal orientation with respect to the primary body axis (14%, n=35) (Figure 1D-E). Thus, *ptk7* limits trunk identity in planarian regeneration.

We next used RNAi and a phenotypic enhancement assay to identify other PCGs that participate with *ptk7* in trunk identity regulation (Figure 1-figure supplement 2). Co-inhibition of *ptk7* with either *wntP-2/wnt11-5/wnt4b* (hereafter referred to as *wntP-2*), *ndl-3*, *Dvl-2* (Almuedo-Castillo et al. 2011), or *fzd-1/2/7* caused the strongest enhancement of the ectopic pharynx phenotype, resulting in 100% of animals affected, whereas co-inhibition with other PCGs affected this phenotype more weakly and below statistical significance under these conditions. *wntP-2* encodes a Wnt gene expressed in a graded fashion from the posterior (Figure 1-figure supplement 2) and based on phylogenetic analyses has been proposed to be either a Wnt11 (Gurley et al. 2010) or Wnt4 (Riddiford and Olson 2011) family member. Planarian *ndl-3* is

expressed in a graded fashion from the anterior (Rink et al. 2009) (Figure 1-figure supplement 2), and encodes a member of the conserved FGFR1/*nou-darake* class of cell-surface molecules that possess an FGF-receptor-like extracellular domain but lacks a tyrosine kinase intracellular domain and are thus proposed to function as FGF signaling inhibitors (Cebrià et al. 2002; Gerber et al. 2009). *fzd-1/2/7* encodes a predicted Wnt receptor expressed broadly (Figure 1-figure supplement 2). Individual inhibition of *ptk7*, *wntP-2*, and *ndl-3* caused formation of ectopic posterior mouths (30/35 *ptk7(RNAi)* animals, 22/33 *wntP-2(RNAi)* animals, 14/23 *ndl-3(RNAi)* animals), and ectopic posterior pharynges (5/35 *ptk7(RNAi)* animals, 8/33 *wntP-2(RNAi)* animals, 2/23 *ndl-3(RNAi)* animals) in amputated animals regenerating both their heads and tails compared to controls (0/46 animals) (Figure 2A). We verified knockdown of *ptk7*, *wntP-2*, and *ndl-3* using in situ hybridizations and qPCR (Figure 2-figure supplement 1A-B). Inhibition of any pairwise combinations of the three genes enhanced the trunk expansion phenotypes (Figure 2A-B) (animals with ectopic pharynges: 45/55 *wntP-2(RNAi);ptk7(RNAi)*, 29/32 *ptk7(RNAi);ndl-3(RNAi)*, 24/40 *wntP-2(RNAi);ndl-3(RNAi)*), with double-RNAi animals also frequently forming two ectopic pharynges (Figure 2A) and co-inhibition of *ptk7* and *wntP-2* producing highest penetrance and expressivity of trunk duplication phenotypes. The orientation of ectopic pharynges was generally oblique, and sometimes inverted, but the majority in all conditions pointed toward the posterior rather than anterior direction (Figure 2C). Live animals with ectopic pharynges were observed during feeding, and the duplicated pharynx could obtain food (Figure 2D, Video 1), suggesting normal functionality of this organ. Taken together, *ptk7*, *wntP-2* and *ndl-3* form a core group of regionally expressed PCGs that jointly suppress trunk identity during posterior regeneration.

wntP-2 and *ptk7* were expressed regionally in the absence of injury, so we examined whether they act only in regeneration or constitutively to regulate trunk regionalization. Prolonged co-inhibition of *wntP-2* and *ptk7* produced animals with an ectopic pharynx, indicating that these genes together restrict trunk identity homeostatically in the absence of injury (Figure 2E). Furthermore, the fact that such animals ultimately formed multiple ectopic mouths extending toward the posterior suggests that graded activities of *wntP-2* and/or *ptk7*, rather than their control of a binary switch in developmental outcomes, could pattern the tail and trunk regions.

We next examined whether trunk suppression mediated by *wntP-2*, *ptk7*, and *ndl-3* was operational in all regeneration contexts, as is the case for several characterized patterning genes in planarians. By contrast, under RNAi conditions that produced an 80-100% penetrant pharynx duplication in regenerating trunk fragments, head and tail fragments from *wntP-2(RNAi);ptk7(RNAi)* animals or *ndl-3(RNAi);ptk7(RNAi)* animals formed only a single *laminin*+ pharynx as did control animals (Figure 2F). Eventually, after prolonged dsRNA feeding after regeneration, such animals could form ectopic pharynges (76 days of RNAi, n=3 of 12 animals examined), consistent with homeostatic functioning of the three genes. However, these results indicate that *ptk7*, *wntP-2* and *ndl-3* suppress trunk expansion in a context-dependent manner and suggest they may provide information about trunk absence or presence during regeneration.

We investigated the anatomy of *ptk7(RNAi);wntP-2(RNAi)* and *ptk7(RNAi);ndl-3(RNAi)* regenerating trunk fragments to determine the extent of the axis under control of the three genes. We first examined the influence of *ptk7*, *wntP-2*, or *ndl-3* inhibition on expression of PCGs and tissue-specific genes marking A-P axial identity (Figure 3A-B). Such *ptk7(RNAi);wntP-2(RNAi)* or *ptk7(RNAi);ndl-3(RNAi)* regenerating animals had normal anterior pole and brain regions (marked by *notum*, *ndk*) and a normal pre-pharyngeal region anterior to the original pharynx (marked by *wnt2* and novel gene *SMU15014980*), expansion of trunk-related peripharyngeal cells (expressing *mmp1*, *FoxA*, and *SMU15007112*), a reduced domain of PCGs expressed in the posterior (*wnt11-1*, *fzd-4-1* and *Abd-Ba*), and normal expression of *wnt1* at the posterior pole. We performed additional examinations of the brain (marked by *chat* and *cintillo*) and far posterior (marked by *wnt11-2*) in *ptk7(RNAi);wntP-2(RNAi)* animals and found no apparent differences compared to control animals (Figure 3-supplement 1A-B). Thus, *ptk7*, *wntP-2*, and *ndl-3* normally promote anterior tail identity at the expense of the trunk and do not strongly affect head or tail formation. Both the pre-existing and ectopic pharynx were capable of regeneration after amputation by sodium azide treatment (Adler et al. 2014), suggesting that *wntP-2/ptk7* signaling acts in part to limit the size of the trunk region within the posterior rather than only functioning to position the anterior extent of newly made trunk tissue (Figure 3C). We next inhibited *ptk7* and *wntP-2* in a regenerating sexual strain of *S. mediterranea* that forms reproductive organs posterior to the pharynx upon attainment of appropriate size. Such animals formed both an ectopic pharynx and ectopic reproductive organs marked by *laminin* and *dmd-1* expression respectively (Chong et al. 2013), indicating *ptk7* and *wntP-2* regulate trunk

regionalization beyond only control of pharynx and mouth formation (Figure 3-figure supplement 1C).

The pharynx is formed from *FoxA*⁺ precursors derived from *smewi-1*⁺ neoblasts. Because inhibition of trunk identity genes produced an ectopic pharynx, we reasoned this structure likely arose from *FoxA*⁺ progenitor cells. Indeed, *ptk7(RNAi);wntP-2(RNAi)* animals regenerating an ectopic pharynx produced an ectopic domain of *FoxA*⁺ cells at a time (7 days of regeneration) prior to appearance of a fully formed ectopic pharynx (14 days of regeneration) (Figure 3C). Expression domains of *ptk7* (Figure 1B) and *wntP-2* (Petersen and Reddien 2009; Gurley et al. 2010) can be altered by amputation independently of neoblasts, so we suggest these genes likely function to regulate axis organization upstream of controlling neoblast fates.

The unidirectional nature of these axis patterning phenotypes as expansion of trunk at the expense of tail identity prompted us to determine more precisely the nature of the regionalized expression of *ptk7*, *wntP-2* and *ndl-3* mRNAs. Visual inspection of colorimetric in situ hybridizations suggested that *ndl-3*, *ptk7*, and *wntP-2* are expressed in overlapping domains along the anteroposterior axis (Figure 4A). We verified this interpretation by quantifying the staining intensity of colorimetric in situ hybridizations along a lateral region running from head to tail (Figure 4B). *ndl-3* staining intensity was maximal in the anterior in a region of graded *ptk7* staining. *ptk7* staining was maximal in the trunk region in which *wntP-2* and *ndl-3* staining form opposing gradients. *wntP-2* staining was maximal in the posterior tail in a region of relatively less *ptk7* expression. The graded expression detected in this manner could arise from regional differences in the abundance of cells that uniquely express each factor or in regulation of cells that express combinations of the three genes. To test these models, we performed triple FISH to simultaneously detect expression of all three genes in eight domains along the head-tail axis, which broadly confirmed the regionalized expression behavior of anterior/pre-pharyngeal maximal *ndl-3* expression, trunk maximal *ptk7* expression, and tail maximal *wntP-2* expression (Figure 4C). We sought to verify this trend quantitatively and segmented the images to examine cells expressing any of the three genes (see Materials and Methods) then determined the mean FISH intensity for each gene per cell. This demonstrated that regions of maximal expression of *ndl-3*, *ptk7*, and *wntP-2* are comprised of cells with high expression of these genes (Figure 4D). We next examined pairwise comparisons of expression of each gene across the body axis (Figure 4E). This approach identified cells that co-express *wntP-2* and *ndl-3* (in particular in head-to

trunk proximal regions R3-R5, Figure 4E), *ptk7* and *ndl-3* (head-to-trunk regions R2-R4), and *ptk7* and *wntP-2* (trunk-to-tail regions R5-R7). We explored whether this approach could identify the spatial distribution of discrete states of cells expressing all combinations of the three genes. We pooled the cell-based expression data across all regions to determine an approximate threshold to define higher versus lower expression for each gene, then assigned each measured cell into one of eight expression classes representing each combination of high versus low expression of each *ptk7*, *wntP-2*, and *ndl-3* and determined their distribution across the head-tail axis (Figure 4-figure supplement 1A-C). This approach identified domains enriched for each expression state, finding a cohort with high *wntP-2* expression and low *ptk7* and *ndl-3* expression in the far posterior, a cohort co-expressing *ptk7* and *wntP-2* in the anterior tail and trunk regions, a cohort only expressing *ptk7* and not *wntP-2* or *ndl-3* centered in the trunk, cohorts of triple-positive cells and *ptk7+ndl-3+* cells in the pre-pharyngeal region, and cohort of *ndl-3+* cells in the anterior. These results suggest that a complexity of PCG cell expression states populate regions of the body axis and that a region of high *wntP-2* and *ptk7* expression exists in the anterior tail at a location where these two genes act together to suppress trunk identity.

We examined the involvement of canonical Wnt signaling on expression of these factors, as this pathway has multiple functions in patterning the primary body axis (Petersen and Reddien 2009). *β-catenin-1* inhibition in uninjured animals severely reduced the expression of *ptk7*, *wntP-2* and *ndl-3* (Figure 5A), consistent with prior analyses of their expression requirements in regeneration (Owen et al. 2015; Reuter et al. 2015). We additionally inhibited *APC*, encoding an intracellular negative regulator of beta-catenin stability and examined regenerating animals for expression of the three trunk regulatory genes (Figure 5-figure supplement 1). Such animals regenerated anterior tails that expressed *wntP-2* throughout, that expressed *ptk7* strongly in a region near the amputation plane and away from the terminus, and that lacked *ndl-3* expression. These results suggest that beta-catenin upregulation can be sufficient for tail axis formation in conjunction with *wntP-2* and *ptk7* expression. Taken together, normal levels of beta-catenin signaling are important for the normal expression of *ptk7*, *wntP-2* and *ndl-3*.

We next examined candidates for signaling that could occur downstream of *wntP-2*, *ptk7*, and *ndl-3*. *Ptk7* proteins can signal through several pathways, including as a coreceptor for Wnt/Frizzled signaling (Lhoumeau et al. 2011). The results of our *ptk7* RNAi enhancement screen suggested a candidate molecular pathway in which *wntP-2* signals through *ptk7* and

fzd1/2/7 to suppress trunk identity. We verified that RNAi of *fzd1/2/7* alone resulted in ectopic mouth and pharynx formation similar to *ptk7* and/or *wntP-2* inhibition (Figure 5-figure supplement 2A). Similarly, we verified that *Dvl-2* but not *Dvl-1* could interact with *ptk7* genetically, suggesting the involvement of *Dvl-2* in trunk suppression (Figure 5-figure supplement 2B). Ptk7 proteins can act in planar cell polarization so we tested for possible functional interactions between *ptk7* and components of the Planar Cell Polarity pathway *vangl1*, *vangl2*, *DAAMI* and *ROCK* but inhibition of these genes did not increase or decrease the occurrence of ectopic mouth or pharynx phenotypes (Figure 5-figure supplement 3). We additionally tested whether a downstream step in trunk suppression could be promotion or inhibition of beta-catenin activity. However, co-inhibition of *ptk7* and *wntP-2* or *ptk7* and *ndl-3* had no detectable effect on expression of beta-catenin-dependent transcripts *axin-B* and *teashirt* (Figure 5B, Figure 5-figure supplement 4A-B) (Owen et al. 2015; Reuter et al. 2015). *β-catenin-1(RNAi)* animals lose trunk regional identity and their pharynx while becoming completely anteriorized (Iglesias et al. 2008), so we tested for possible functional interactions between beta-catenin signaling and trunk control genes by inhibiting *ptk7/wntP-2* along with *APC*. We could not detect any enhancement or suppression of ectopic pharynx formation in that assay, further suggesting independence between *ptk7/wntP-2* and *APC/β-catenin-1* signaling (Figure 5-figure supplement 4C). These observations are consistent with the clear distinction between the *β-catenin-1* RNAi phenotype of ectopic head production (Gurley et al. 2008; Iglesias et al. 2008; Petersen and Reddien 2008) as compared to the *ptk7(RNAi);wntP-2(RNAi)* and *ptk7(RNAi);ndl-3(RNAi)* phenotypes of ectopic trunk formation without affecting the identity of the anterior and posterior poles. Together, these results strongly suggest that trunk regionalization can be separable from pole identity and that *ptk7* and *wntP-2* likely do not operate exclusively through *β-catenin-1* to pattern the trunk and tail.

Regeneration can involve the re-definition of positional identity within pre-existing tissues, but the mechanisms controlling this process are unclear. We examined the expression and activities of *ptk7*, *wntP-2*, and *ndl-3* in forming a mouth and pharynx (expressing *laminin*) within the pre-existing tail tissue (Figure 6B). In amputated tail fragments, the mouth and pharynx were formed during the first 5 days of regeneration, with expression of *laminin* evident as early as 3 days. *wntP-2* was initially expressed throughout the amputated tail, but its expression restricted posteriorly starting around day 2, reaching a minimum around day 4, and

re-establishing to intact proportions around day 7 (Petersen and Reddien 2009; Gurley et al. 2010). *ndl-3* expression was initially absent in the tail fragments, emerged at day 1 in the far anterior then spread posterior to occupy the anterior half of the regenerating fragments by 4 days. *ptk7* expression remained broad in tail fragments through early times in regeneration and re-established a trunk-proximal domain evident by 7 days. Notably, the position of the newly regenerated pharynx correlated with a domain in which *wntP-2* expression was reduced and *ndl-3* was elevated.

We next examined the functions of *ptk7*, *wntP-2* and *ndl-3* in positional information control within regenerating tail fragments. In tail fragments, inhibition of *ptk7* caused a posterior shift to the location of the mouth and pharynx (Figure 6A, Figure 6-figure supplement 1A), an effect enhanced by co-inhibition of *wntP-2* or *ndl-3* though not caused by *wntP-2* or *ndl-3* inhibition alone (Figure 6-figure supplement 1B). Reduced doses of *wntP-2* and *ptk7* dsRNA resulted in intermediate placement phenotypes, and the distributions of placement phenotypes were not biphasic (Figure 6-figure supplement 1C), suggesting the activity of these genes could regulate pharynx position in a graded fashion rather than controlling a switch between two alternate organ locations. *ptk7(RNAi);wntP-2(RNAi)* tail fragments regenerated with posteriorly restricted expression of *fzd4-1* and *wnt11-1* and posteriorly expanded expression of *sFRP-2*, without strongly affecting the positioning of the brain (*ndk*) or pre-pharyngeal regions (*SMU15014980*) (Figure 6-figure supplement 2D). Together, these experiments suggest that *ptk7*, along with *wntP-2* and *ndl-3*, has a primary activity in controlling the positioning of trunk/tail tissues in regeneration.

To examine the relationship between the expression and function of *ptk7* and *wntP-2* signaling in regional identity re-establishment, we analyzed the time of emergence and critical time for pharynx placement phenotypes in regenerating tail fragments. RNAi of *ptk7* for three days prior to tail amputation resulted in a posterior shift in the location of the newly formed *laminin* expression domain detected as early as 3 days of regeneration (Figure 6-figure supplement 2A). These results indicate that *ptk7* acts before day 3 of regeneration. To determine a lower bound for the latest time of action for trunk control genes, we performed timed delivery of dsRNA via injections performed at successive two-day intervals during regeneration then examined the position of the *laminin* expression domain 7 days after amputation. Injections of *wntP-2* and *ptk7* dsRNA only prior to amputation, or as late as day 1 and day 2, were capable of

posteriorly shifting the *laminin* expression domain (Figure 6-figure supplement 2B). Taken together, these results suggest that *ptk7/wntP-2* signaling has functions in pharynx positioning after day 1 and before day 3, coinciding with the timing of *wntP-2*'s posterior restriction and *ndl-3*'s anterior expression. This occurs prior to the ultimate reestablishment of *ptk7*, *wntP-2* and *ndl-3* expression into finalized trunk, posterior, and anterior domains by 7-14 days, suggesting a separation between processes that control initial organ placement and ultimate proportion restoration (Figure 6A).

The coordinate regulation of *wntP-2* and *ndl-3* in regeneration led us to examine candidate transcriptional interactions among *wntP-2*, *ndl-3*, and *ptk7*. We did not detect strongly apparent changes to these expression domains after single inhibition of the other two genes by WISH, FISH or qPCR (Figure 6-figure supplement 3A-C). We tested for possible mutual expression requirements in tail fragments, reasoning this might provide a sensitized context in which the expression domains normally undergo regulation. *wntP-2* expression was reduced in *ndl-3(RNAi)* tail fragments, particularly along the lateral edges (Figure 6C), and posteriorly restricted in *ptk7(RNAi)* regenerating tail fragments (Figure 6-figure supplement 4A), suggesting that these genes can normally promote expression of *wntP-2* in regenerating tail fragments. By contrast, *ndl-3* expression was expanded posteriorly in *ptk7(RNAi)* and *ptk7(RNAi);wntP-2(RNAi)* tail fragments (Figure 6D, Figure 6-figure supplement 4B). We inhibited *ptk7* and *wntP-2* in uninjured animals to determine whether this effect was specific for regenerating tail fragments. Such animals expressed *ndl-3* ectopically posterior to the pharynx at a time (by 12 days of homeostatic RNAi) prior to significant pharynx formation (Figure 6E-F, Figure 6-figure supplement 3A-B). Analysis of these ectopic *ndl-3*⁺ cells by double-FISH revealed that the majority (41/63) co-expressed *collagen* and were located within the plane of the body-wall musculature (Figure 6F). These observations argue for a specific regulatory relationship in which *ptk7* and *wntP-2* together suppress expression of *ndl-3* in the posterior. Alternatively, the nascent pharynx could exert influence over the expression of *ndl-3* in a manner indirectly controlled by *ptk7* and *wntP-2*'s suppression of pharynx identity. Together these experiments indicate *ptk7*, *wntP-2* and *ndl-3* can directly or indirectly engage in regulatory interactions in homeostatic maintenance of tissue pattern and also in re-establishment of pattern in regeneration.

Discussion

These experiments suggest a molecular model in which trunk identity and axis position are determined by low *wntP-2* activity signaling through the co-receptor *ptk7* and receptor *fzdl/2/7*, which together could provide competence for beta-catenin-independent outputs necessary for trunk and anterior tail patterning (Figure 7A). *ndl-3* is expressed in the trunk region yet acts with the same sign as *wntP-2* and *ptk7* to suppress posterior trunk expansion, either through a parallel or downstream process engaged in trunk suppression (Figure 7A) or perhaps due to its ability under some circumstances to promote robust expression of *wntP-2* (Figure 6C). In the tail region of uninjured animals and regenerating trunk fragments, high levels of *wntP-2/ptk7* activity prevent the acquisition of trunk identity and enable the formation of anterior tail tissue (Figure 7B). By contrast, head fragments initially have lower expression of *wntP-2* and *ptk7*, which could facilitate their formation of trunk tissue through regeneration. Amputated tail fragments would be expected to initially possess high levels of *wntP-2* and *ptk7* activity, but a regeneration expression regulatory program reduces *wntP-2* mRNA from the anterior to allow trunk regionalization to occur at an appropriate location. These models suggest that the expression status of *wntP-2* and *ptk7* could provide information about the presence or absence of pre-existing tissues used in determining regeneration outcomes. A previously proposed animal-wide gradient of β -catenin-1 activity (Reuter et al. 2015) could set up the axis into distinct *ptk7*, *wntP-2* and *ndl-3* expression domains refined by *wntP-2* and *ptk7* repression of *ndl-3* expression. However, our experiments argue that a β -catenin-1-independent signaling output downstream of *wntP-2* and *ptk7* likely act to suppress trunk regional identity and thereby control placement of a trunk/tail boundary along the axis according to a gradation of their activities within the posterior. The identification of trunk expansion phenotypes independent of head/tail identity transformations suggests that whole-body regeneration involves a regulatory hierarchy of anterior/posterior pole formation followed by subsequent regional subdivision.

Our results thus establish a link between Wnt, Ptk7 and FGFR proteins in regeneration patterning and axis formation. In mice and zebrafish, Ptk7 deletion causes defects in axis formation including a lack of convergent extension within the trunk and tail and a mispolarized auditory epithelium in mice, similar to disruption of core planar cell polarity components that signal independently of beta-catenin (Lu et al. 2004; Hayes et al. 2013). However, studies in *Drosophila*, zebrafish, *Xenopus* and mammalian tissue culture have found conflicting evidence

that Ptk7 can also either promote (Puppo et al. 2011; Bin-Nun et al. 2014) or inhibit (Peradziryi et al. 2011; Hayes et al. 2013) beta-catenin-dependent signaling in a context-dependent manner. The regional identity defects we observe after *ptk7* RNAi in planarians are not obviously the result of defective planar cell orientations, are phenocopied by inhibition of a Wnt gene, and do not globally affect beta-catenin transcriptional targets or beta-catenin-dependent processes. We suggest that Ptk7 proteins can control tissue fate through an alternate mechanism, perhaps by coordinating the activities of cell cohorts within a field. Planarians and most other animals have expression of multiple Wnts in posterior domains, pointing to their ancient use in organizing the primary body axis (Petersen and Reddien 2009). The use of Ptk7 proteins for trunk/tail regionalization could therefore have an ancient origin and allow posterior Wnts to produce distinct signaling outcomes for combinatorial pattern control.

We also find with *wntP-2* and *ndl-3* a second example in planarians of shared patterning regulation between Wnt and FGFR1 factors. Whereas *wntP-2/wnt11-5/wnt4b* and *ndl-3* restrict the domain of the trunk, *wntA/wnt11-6/wnt4a* (Kobayashi et al. 2007) and *nou darake* (Cebrià et al. 2002) restrict the domain of the head and brain. Intriguingly, in both cases, the FGFR1 genes have most prominent expression in the anterior but act with the same sign as the Wnt genes to promote more posterior identity outside of the domain of their own expression. In mammals, FGFR1 and Wnt4 are each required for formation of the metanephric kidney from intermediate mesoderm, suggesting this positive regulatory relationship is conserved (Stark et al. 1994; Gerber et al. 2009).

Pattern restoration in regeneration has been proposed to involve intercalation (French et al. 1976) or progressive specification of adjacent regions (Roensch et al. 2013) to restore positional values across a field disrupted by amputation. In planarians, asymmetric wound-induced expression of *notum* provides information about wound site directionality used to program anterior-versus-posterior pole fates (Petersen and Reddien 2011). By contrast, we find genes encoding signaling molecules that are constitutively expressed in body-wide mRNA gradients and are used for control of positional information in regeneration. Graded expression of paracrine factors across fields of cells could enable patterning over the large length-scales necessary for adult regeneration. The interactions between this tissue-wide positional information present at the time of injury, combined with wound-induced directional cues, could account for robust pattern control in regeneration.

403

404 **Acknowledgements**

405 We thank members of the Petersen lab for helpful discussions and E. Hill for the *ndl-3* plasmid.

406

407

408

409

410

411

412

413

414

415

416

417

418

419

420

421

422

423

424

425

426

427

428

429

430

431

432

433

Figure legends

Figure 1. *ptk7* is a positional control gene that suppresses trunk identity in regenerating

planarians. (A) Left panel, Double FISH to detect coexpression of *ptk7* within *collagen*⁺ cells of the body-wall musculature in a trunk-centered gradient (116/125 *collagen*⁺ cells were *ptk7*⁺ and 113/125 *ptk7*⁺ cells were *collagen*⁺, scored in ventral prepharyngeal subepidermal region). Right panels, higher magnification of *collagen*⁺*ptk7*⁺ cells. (B, upper panels) Freshly amputated head fragments have *ptk7* expression in the CNS but minimal levels in subepidermal cells but by 48-96 hours expression appears at a region within the new anterior of the fragment (arrows, anterior extent of *ptk7* expression). (B, lower panels) Animals treated with lethal doses of gamma irradiation (6000 Rads) three days prior to amputation undergo a similar re-establishment of a *ptk7* expression domain along the A-P axis. Images represent at least 3/3 animals probed. (C) Irradiation controls showing elimination of *smedwi-1*-expressing neoblasts in animals from the same cohort as (B). (D) Animals were injected with control or *ptk7* dsRNA three times over three days, amputated to remove heads and tails, allowed to regenerate, fixed at 14 days and stained with a *laminin* riboprobe detecting both the mouth and pharynx (left panels, dotted line indicates amputation plane, red box shows enlarged region of *ptk7*(RNAi) animals) or stained with Hoechst dye to label nuclei and visualize the pharynx (right). *ptk7* RNAi caused formation of an ectopic posterior mouth in regenerating trunk fragments (28/35 animals), but not in regenerating head or tail fragments (35/35 animals each). (D, right) More rarely, *ptk7* inhibition caused formation of an ectopic posterior pharynx. (E) Control or *ptk7*(RNAi) animals stained with a fluorescent lectin Concanavalin A to visualize the epidermis and the pre-existing or ectopic mouth (red arrow). Bars, 25 (A), or 200 (B), or 400 microns (D-E).

Figure 2. *ptk7* acts with *wntP-2* and *ndl-3* to suppress trunk identity in a context-dependent

manner. (A) *ptk7*, *wntP-2*, and *ndl-3* dsRNAs were fed to animals individually or in pair-wise combinations prior to amputation to remove heads and tails, fixation 25 days later, staining with a *laminin* riboprobe and Hoechst dye. (B) Scoring information for pharynx and mouth

duplication phenotypes. Animals were scored for presence of ectopic mouth (defined as a superficial circle of *laminin*⁺ cells which was always present posterior to the original mouth, arrow), and ectopic pharynx (defined as having pharynx morphology by *laminin*⁺ and Hoechst⁺ staining, double arrows) and its orientation with respect to the A-P body axis. Animals with an ectopic mouth but not a fully formed ectopic pharynx often had varying degrees of internal *laminin* expression suggestive of a growing pharynx primordium and were scored as having an ectopic mouth only. Co-inhibition of any pairwise combination of the three genes enhanced the penetrance and expressivity of the ectopic pharynx phenotypes. Note that combined pairwise inhibition of *ptk7*, *wntP-2* and *ndl-3* enhanced the trunk duplication phenotype and that dual inhibition of *ptk7* and *wntP-2* produced the strongest effects. (C) Analysis of ectopic pharynx orientation, measured at the proximal end of the ectopic pharynx. In many cases, the ectopic pharynx was oriented at an oblique angle with respect to the body axis, perhaps as a result of ectopic mouth placement nearby the original mouth, and ectopic pharynges were observed with fully inverted polarity. In all animals that formed 2 ectopic pharynges (derived from pairwise combinations of dsRNAs), both structures were oriented toward a common ectopic mouth located along the posterior midline. (D) Images of live animals showing the ectopic pharynx in *ptk7(RNAi);wntP-2(RNAi)* animals (red arrow) can be functional for feeding. (E) Prolonged inhibition of *ptk7* and *wntP-2* in uninjured animals for at least 36 days (64 days shown) caused formation of an ectopic pharynx (6/8 animals) and multiple posterior mouths (8/8 animals). (F) Inhibition of *ptk7* and *wntP-2* or *ptk7* and *ndl-3* caused head and tail fragments to regenerate only a single pharynx like control animals. Therefore, the effects of *ptk7*, *ndl-3* and *wntP-2* in body patterning are context dependent. Anterior, left. Bars, 300 (A,E) or 500 (F) microns.

Figure 3. *ptk7*, *wntP-2* and *ndl-3* control tail-versus-trunk identity. (A) In situ hybridizations to detect A-P tissue regionalization in control and *ptk7(RNAi);wntP-2(RNAi)* and *ptk7(RNAi);ndl-3(RNAi)* regenerating trunk fragments fixed 21 days after head and tail amputation, marking the anterior and head region (*ndk*, *wnt2*), prepharyngeal region (novel gene SMU15014980), trunk (novel gene SMU15007112, *mmp1*, *foxA*), posterior (*wnt11-1*, *fzd4-1*, *Abd-Ba*), and the anterior and posterior poles (*wnt1*, *notum*). All panels represent 100% of at least 6 animals stained. Arrow, ectopic trunk gene expression. Brackets, decrease in size of tail

domain. (B) Quantitation of domain size changes from experiments described in (A), measured as length of domain normalized to body length. *ptk7(RNAi);wntP-2(RNAi)* and *ptk7(RNAi);ndl-3(RNAi)* regenerating trunk fragments had increased sizes of trunk domains marked by expression of *mmp1*, *foxA* and SMU15007112, and decreased sizes of tail domains marked by expression of *wnt11-1* and *fzd4-1* with little to no change to other domains. Asterisks, $p < 0.05$ by 2-tailed t-test. (C) Both the pre-existing and ectopic pharynx in *wntP-2(RNAi);ptk7(RNAi)* animals regenerated (4/4 animals) after amputation with brief sodium azide treatment, using FISH to mark the gut (*porcupine*, green) and mouth and pharynx (*laminin*, red). Asterisk, pre-existing pharynx; arrows, ectopic pharynx, arrowhead, ectopic mouth. (C) *ptk7(RNAi);wntP-2(RNAi)* animals form ectopic *FoxA*⁺ cells by day 7 of regeneration. Bars, 100 (D), 200 (A), or 300 (C) microns.

Figure 4. *ndl-3*, *ptk7*, and *wntP-2* are expressed in a graded fashion in domains along the anteroposterior axis. (A) In situ hybridizations showing body-wide graded expression of *ptk7* centered in the trunk, *wntP-2* expression in a gradient from the posterior and *ndl-3* expression in a graded fashion from the anterior. (B) Quantitation of colorimetric in situ hybridization staining across the body axis. 4-6 planarians stained as in (A) were imaged on a dissecting microscope, the images were inverted and then analyzed for position-specific staining intensity along a lateral domain depicted in the diagram (dotted line with arrow showing directionality). To compare animals of different lengths, position was normalized to length of this domain and signal intensity was normalized such that the minimum and maximum values across each animal were 0 and 1, respectively, and average intensity at each region was determined for animals stained with each probe treatment computed followed by obtaining average intensity, with bars showing standard deviations. (C) Triple FISH showing expression of *ndl-3* (red), *ptk7* (blue), and *wntP-2* (green) mRNA. Panels are maximum projections from a stack of seven 1-micron thick confocal images taken at 40x along the body axis at the regions represented in the cartoon, then adjusted for brightness and contrast uniformly for each channel across the image series. m, mouth. Bars, 100 microns. (D-E) Quantification of FISH signal intensity for cells identified in images shown in (C). 3-color images were segmented by merging all three channels to define a set of cells in each region with *wntP-2*, *ndl-3* and/or *ptk7* expression and this mask used to measure mean FISH

signal intensity for each cell. (D) Scatter and box plots showing expression of *ndl-3* highest in the anterior, expression of *ptk7* highest in the trunk and tail, and highest *wntP-2* expression in the posterior. (E) Plots comparing pairwise FISH signal intensity between the indicated genes across eight body axis regions (R1-R8) as in (C). Note the existence of cells expressing both *ndl-3* and *wntP-2* (R3-R5), *ptk7* and *ndl-3* (R3-R4), and *wntP-2* and *ptk7* (R5-R7). Bars, 100(C) or 200 (A) microns.

Figure 5. Trunk control genes likely signal independently of β -catenin-1. (A) In situ hybridizations show reduced expression of *ptk7* (11/11 animals), *wntP-2* (6/6 animals), and *ndl-3* (6/6 animals) after 8 days (*wntP-2*, *ndl-3*) or 19 days (*ptk7*) of β -catenin-1 RNAi in uninjured animals. (B) In situ hybridizations showing reduction of *axin-B* expression after 11 days of β -catenin-1 RNAi (14/14 animals) but not after inhibition of *wntP-2* and *ptk7* (14/14 animals) or *ndl-3* and *ptk7* (14/14 animals). Bars, 400 microns.

Figure 6. *ptk7* acts with *wntP-2* and *ndl-3* to specify trunk position in regeneration. (A) In situ hybridizations of regenerating tail fragments showing that pharynx formation (marked by *laminin* expression) coincides with early reduction of *wntP-2* expression and increase in *ndl-3* expression. *ptk7* is expressed broadly and re-establishes a trunk-centered gradient by 7 days. All images represent at least 4/4 animals probed except *laminin* (d0) and *ptk7* (d0, d3 and d4) representing 3/3 animals probed. (B) *ptk7(RNAi);wntP-2(RNAi)* animals form a single pharynx located too far posteriorly (7/8 animals, quantification in Figure 6-figure supplement 1A-B). (C) *wntP-2* expression is reduced in *ndl-3(RNAi)* regenerating tail fragments (10/14 animals). (D-E) *ndl-3* expression is expanded posteriorly in (D) *ptk7(RNAi);wntP-2(RNAi)* regenerating tail fragments by 7 days after amputation (4/5 animals) and in (E) intact animals after 12 or 17 days of RNAi (25/28 animals). (F) Control or *ptk7(RNAi);wntP-2(RNAi)* animals were stained for *ndl-3* and *collagen* expression after 17 days of RNAi and optical sections were imaged of the body-wall musculature in the region posterior to the pre-existing pharynx. Simultaneous inhibition of *ptk7* and *wntP-2* increased the frequency of *ndl-3+collagen+* cells versus total *ndl-3+* cells found in the tail region (41 of 63 cells in *ptk7(RNAi);wntP-2(RNAi)* animals versus 7 of 32 cells scored in control animals, $p < 0.0001$ by Fisher's exact test). (G) Model for function of *wntP-2*, *ptk7* and *ndl-3* in regeneration patterning and positional identity. The highest co-expression of

wntP-2 and *ptk7* occurs in the anterior tail and trunk at a location where these genes suppress trunk fates. *wntP-2* and *ptk7* acting in this region prevent trunk fates in animals undergoing tissue homeostatic maintenance and in regenerating trunk fragments that form new tail tissues. By contrast, regenerating head fragments lack abundant co-expression of *wntP-2* and *ptk7*, which we suggest is important for enabling the normal regeneration of new trunk regionalization. Regenerating tail fragments would be expected to initially possess high levels of *wntP-2* and *ptk7*. A regeneration expression regulatory program reduces *wntP-2* expression in this region, enabling trunk regeneration at a position that we suggest could be defined by a particular A-P location of *ptk7* and *wntP-2* activity present at an appropriate time in regeneration. *wntP-2* and *ptk7* can inhibit *ndl-3* expression in the posterior, and *ndl-3* promotes *wntP-2* expression but could also act in parallel through an unknown mechanism to suppress trunk identity. β -catenin-1 signaling is required upstream for expression of *ptk7*, *wntP-2* and *ndl-3*. Reduced *wntP-2/ptk7* activity in the middle of the animal enables trunk formation. Bars, 200 (A-D) or 400 (E) microns.

Video 1. Ectopic pharynges in *ptk7(RNAi);wntP-2(RNAi)* animals can be functional for feeding, related to Figure 2. Movie of a live *ptk7(RNAi);wntP-2(RNAi)* animal showing both the original and ectopic pharynges in a 21 day regenerating trunk fragment feeding on liver paste.

Supplemental Figure legends

Figure 1-figure supplement 1. Sequence alignment of *Smed-ptk7*.

Alignment of predicted protein sequence of *Smed-ptk7* with human (HsPtk7, NP_002812.2), mouse (MmPtk7, AAH76578.1), *Xenopus laevis* (XlPtk7, NP_001083315.1), zebrafish (DrPtk7, AGT63300.1) and *Drosophila melanogaster* (otk, AAF58596.1) Ptk7 proteins. SMED-PTK7 is predicted to have 7 extracellular Ig-family domains and an intracellular tyrosine kinase domain (<http://smart.embl-heidelberg.de>).

Figure 1-figure supplement 2. RNAi enhancement screen identifies modulators of *ptk7* activity involved in trunk patterning.

(Upper) Plot of ectopic posterior pharynx phenotype penetrance after administration of dsRNA targeting *ptk7* and each of 22 previously identified positional control genes or Wnt-related factors expressed regionally along the body axis (*wnt11-1*, *wnt11-2*, *wnt11-4*, *wntP-2*, *wnt2-1*, and *wnt5*), general intracellular components of Wnt signaling (frizzled receptors expressed in the posterior: *fzd4-1/fzd4*, *fzd4-2*, and *fzd1/2/7*; Disheveled proteins: *Dvl-1* and *Dvl-2*), downstream components of Wnt signaling that act positively (*teashirt*) or negatively (*axin-B*) to influence β -catenin-1 signaling, secreted Wnt inhibitors (*sFRP-1*, *sFRP-2*, *sFRP-3*, *notum*), Wnt-PCP pathways (*DAAM1*, *ROCK*, *vangl2*), and FGFR-like/*nou-darake* family factors (*ndl-3*, *ndl-4*). At least 5 animals were examined in each condition except for *wntP-2*, *DAAM1*, *ROCK*, *vangl2* RNAi treatments in which at least 24 animals were examined. Asterisks indicate $p < 0.05$ from Fisher's exact test versus control + *ptk7* dsRNA treatment after Benjamini-Hochberg correction for false discovery. Inhibition of *ptk7* along with either *wntP-2* ($p=5.16E-14$), *ndl-3* ($p=1.24E-05$), *fzd-1/2/7* ($p=0.046$), or *Dvl-2* ($p=4.18E-06$) caused the strongest occurrence of the ectopic pharynx phenotype. (Lower) in situ hybridizations showing regionalized expression of selected genes from the screen.

Figure 2-figure supplement 1. Verification of RNAi knockdown for *ptk7*, *wntP-2* and *ndl-3*.

(A) In situ hybridizations verifying that dsRNA to *ptk7*, *wntP-2*, and *ndl-3* individually reduced the expression of each gene after 12 days of RNAi in the absence of injury (*ptk7*) or 20 days

regeneration after head and tail amputation (*wntP-2* and *ndl-3*) of RNAi. Images represent 100% of animals stained, $n > 4$. Bars, 500 microns. (B) qPCR showing knockdown of *ptk7*, *wntP-2* and *ndl-3* mRNA. Asterisks indicate $p < 0.05$ by a 2-tailed t-test.

Figure 3-figure supplement 1. Additional histological analysis of *ptk7(RNAi);wntP-2(RNAi)* and animals. (A) In situ hybridizations as in 2A showing normal expression of *chat*, *mag-1*, and *wnt111-2*, but reduced expression domain of *fzd-4-1* in *ptk7(RNAi);wntP-2(RNAi)* animals 18 days after head and tail amputation. (B, left) Co-inhibition of *ptk7* and *wntP-2* did not affect numbers of *cintillo*+ neurons of the lateral brain region in day 21 regenerating head fragments or trunk fragments, (B, right) with quantifications of cell number normalized to animal area. Anterior, top. (C) Control sexual strain animals regenerate to have a single pharynx (asterisk, *laminin* expression) and a penis papilla (double arrow, *dmd-1* expression) within the trunk (8/8 animals), whereas *ptk7(RNAi);wntP-2(RNAi)* animals regenerated to form an ectopic *laminin*+ pharynx (arrow, 7/7 animals) and ectopic *dmd-1*-expressing tissues (3/7 animals). Bars, 400 microns.

Figure 4-figure supplement 1. Distribution of *ptk7*, *wntP-2* and *ndl-3* expression states across the body axis. (A) Mean fluorescence intensity of cells from all regions in Figure 4C were combined and density histograms plotted to determine a cutoff (dotted line=55 in arbitrary units) for higher versus lower expression of *ptk7*, *wntP-2*, and *ndl-3*. Cells within each region shown in Figure 4C were assigned membership in one of eight classes defined by high (“hi”) or low (unstated) expression of each of the three genes (1: *wntP-2*^{hi} only, 2: *ptk7*^{hi}*wntP-2*^{hi}, 3: *ptk7*^{hi} only, 4: *ptk7*^{hi}*wntP-2*^{hi}*ndl-3*^{hi}, 5: *ptk7*^{hi}*ndl-3*^{hi}, 6: *wntP-2*^{hi}*ndl-3*^{hi}, 7: *ndl-3*^{hi}, 8: all 3 genes low). Class membership was plotted as a fraction of all cells measured in each region (B) and as a scatterplot of all cells examined (C). By these criteria, several classes of cells expressing combinations of *ptk7*, *wntP-2*, and *ndl-3* exist and are distributed in domains along the body axis. The tail tip has the highest frequency of *wntP-2*+ only cells, whereas anterior tail and trunk regions have a comparatively greater fraction of *wntP-2*+*ptk7*+ cells. The above analysis was repeated for a range of high/low expression cutoffs between 30 and 75, resulting in similar the same trends, with lower thresholds resulting in fewer cells assigned as *ptk7*^{lo}*wntP-2*^{lo}*ndl3*^{lo} and more cells as *ptk7*^{hi}*wntP-2*^{hi}*ndl-3*^{hi}.

Figure 5-supplement 1. Examining the effect of *APC* RNAi on expression of *ptk7*, *wntP-2*, and *ndl-3*. *APC(RNAi)* regenerating animals formed a domain of ectopic *ptk7* (8/8 animals) and *wntP-2* (9/9 animals) expression in the anterior tail. The ectopic tail appears to have a domain expressing *wntP-2* and not *ptk7* at the terminus and a domain expressing both *ptk7* and *wntP-2* near the amputation site. Such animals form an ectopic anterior pharynx likely as the consequence of tail formation, and this expressed *ndl-3*, *ptk7*, and *wntP-2*. Bars, 400 microns.

Figure 5-figure supplement 2. *fzd1/2/7* and *dvl-2* inhibition causes ectopic pharynx and mouth formation in the posterior. The indicated dsRNA was delivered to animals by injection prior to amputation, 23 days of regeneration and staining for *laminin* expression to detect pharyngeal tissues. *fzd1/2/7* inhibition (4/6 animals) caused formation of an ectopic pharynx similar to *ptk7*, *wntP-2* and/or *ndl-3* inhibition. *dvl-2* dsRNA enhanced the *ptk7* ectopic pharynx phenotype (9/9 animals). Bars, 300 microns.

Figure 5-figure supplement 3. Testing Planar Cell Polarity genes for involvement in trunk patterning. Regenerating trunk fragments undergoing RNAi as indicated and stained by FISH with a *laminin* riboprobe to detect the pharynx and mouth. Inhibition of *ptk7* along with *vangl1* (8/8 animals), *vangl2* (4/4 animals), *DAAM1* (6/6 animals) and *ROCK* (6/6 animals) did not suppress or enhance defects due to *ptk7* inhibition alone. Bars, 300 microns.

Figure 5-figure supplement 4. *ptk7*, *wntP-2*, and *ndl-3* inhibition do not influence *axin-B* expression and are not modified by *APC* inhibition. (A) qPCR detecting expression of *axin-B* normalized to *ubiquilin* on RNA purified from day 10 regenerating animals after the indicated dsRNA treatments. *β-catenin-1* inhibition reduced relative *axin-B* mRNA abundance, but *ptk7*+*wntP-2* dsRNA and *ptk7* + *ndl-3* dsRNA had no effect. (B) *ptk7*+ *wntP-2* RNAi did not alter expression of the *β-catenin-1* target gene *teashirt* in animals 18 days after head and tail amputation (3/3 animals). (C) APC inhibition did not detectably affect the frequency of ectopic pharynx formation due to *ptk7* and *wntP-2* RNAi (p=1.000, Fisher's exact test) (animals that regenerated an ectopic pharynx: 0/10 control fragments, 0/10 *APC(RNAi)* fragments, 7/9

ptk7(RNAi);wntP-2(RNAi);control(RNAi) fragments and 7/10 *ptk7(RNAi);wntP-2(RNAi);APC(RNAi)* fragments). Bars, 200 microns. Anterior, top.

Figure 6-figure supplement 1. *ptk7*, *wntP-2* and *ndl-3* participate in positioning the pharynx during tail fragment regeneration. (A) Assay design used to measure pharynx position in (B-D) (B) Quantification of pharynx mispositioning defect shown in Figure 4B by measuring the distance from the tail tip to the *laminin*⁺ expression domain normalized to animal length in day 7 regenerating tail fragments after the indicated treatments. (C) Quantification of pharynx placement phenotypes in 7 day regenerating tail fragments after inhibition of *wntP-2*, *ptk7* and *ndl-3* singly or in pairwise combinations as indicated. The strongest effects were observed after simultaneous inhibition of *ptk7* and *wntP-2* or *ptk7* and *ndl-3*. Bars, averages; asterisks indicate $p < 0.05$ by 2-tailed t-test. (D) Dilution of *ptk7*+*wntP-2* dsRNA with control dsRNA caused a progressively weaker pharynx placement phenotype, suggesting a gradation of their activities affect trunk position. (E, left) *ptk7(RNAi);wntP-2(RNAi)* animals stained with riboprobes to several regionally expressed genes shows such animals form normal anterior and prepharyngeal regions, but have posteriorly shifted trunk and tail gene expression domains quantified in (E, right). Graphs show averages of at least 7 samples, error bars show standard deviations, and asterisks indicate $p < 0.05$ by two-tailed t-test. (F) Regenerating *ptk7(RNAi);wntP-2(RNAi)* head fragments form a single pharynx with number of animals scored as indicated. Bars, 200 microns.

Figure 6-figure supplement 2. Determining critical period for *ptk7/wntP-2* signaling in pharynx placement. (A) Measurements of pharynx position as in Figure 4-figure supplement 2A at selected days after amputation in regenerating control or *ptk7(RNAi)* regenerating tail fragments treated with dsRNA for three days prior to amputation or (B) injected with control or both *wntP-2* and *ptk7* dsRNA only at the indicated days with respect to the day of amputation (day 0). Injection of *wntP-2*+*ptk7* dsRNA as late as 1-2 days after amputation can posteriorize the position of the regenerated pharynx. Graphs show averages of at least 4 samples, error bars show standard deviations, and asterisks indicate $p < 0.05$ by two-tailed t-test. Bars, 200 microns.

Figure 6-figure supplement 3. Examining the influence of *ptk7*, *wntP-2* and *ndl-3* on each other's expression. (A-C) Examining intact animals for regulatory interactions among trunk control genes. Uninjured animals fed with the indicated dsRNAs for two weeks prior to fixation and staining by (A) WISH or (B) FISH to examine effects on expression of *ptk7*, *wntP-2* or *ndl-3*. No treatment caused strongly increased or reduced expression except for *ptk7*+*wntP-2* RNAi which caused ectopic expression of *ndl-3* in the anterior tail region (A, 5/8 animals; B, 12/15 animals). (C) Animals were treated with dsRNA as in A and B, then analyzed by qPCR for expression changes to *ptk7*, *wntP-2*, and *ndl-3* following RNAi. Inhibition of each gene caused similar knockdown in either single or double-RNAi contexts. *wntP-2* RNAi caused a weak but statistically significant reduction to *ptk7* transcript levels, similar to WISH detection (A). *fzd1/2/7* RNAi did not significantly alter expression of *ptk7*, *wntP-2*, or *ndl-3*. Bars, 400 microns (A), 300 microns (B).

Figure 6-figure supplement 4. Measurements of the influence of trunk control genes on *wntP-2* and *ndl-3* expression in tail fragment regeneration. (A-B) Animals were treated with the indicated dsRNAs for three days prior to amputation, regenerating tail fragments were fixed 7 days later, and stained for (A) *wntP-2* expression or (B) *ndl-3* expression. Measurements were made from the posterior tip of the regenerating animal to (A) the anterior edge of *wntP-2* expression or (B) the posterior edge of *ndl-3* expression then normalized to animal length. Graphs show averages and error bars are standard deviations. Asterisks indicate $p < 0.05$ by a 2-tailed t-test. Bars, 200 microns.

Materials and Methods

Planarian culture and irradiation treatments

Asexual and sexual strain *Schmidtea mediterranea* were maintained in 1x Montjuic salts between 18-20° C. Gamma irradiation (6,000 Rads) was performed with a Cesium-137 source irradiator at least 24 hours prior to amputation to eliminate all dividing cells.

Gene Sequences

Smed-protein tyrosine kinase-7 (ptk7) was identified through homology searches through BLAST on a planarian transcriptome database (Planmine, <http://planmine.mpi-cbg.de>) identifying a *Schmidtea mediterranea ptk7* homolog dd_Smed_v6_6999_0_1. *Smed-wntP-2* was described previously and cloned using primers 5'-TTAAATGTTCTAAGCCAAAACAACA-3' and 5'-AAAACCTTTTATGATCAATCTGAATGC-3' (NCBI accession number: EU29663) (Petersen and Reddien 2009). *Smed-ndl-3* was cloned using primers 5'-TTATTGACAGTAGGAACCAAAGCC-3' and 5'-ATCCTGAATCAAGTCAACGCCA-3' for dsRNA and riboprobe synthesis as described (Rink et al. 2009). Unless otherwise noted, riboprobes for a 4313-bp fragment of *ptk7* were made from a PCR product cloned by RT-PCR into pGEM-T-easy vector using the primers 5'-GTACTACCTGCCGAAAGTATACA-3', 5'-GCGCATATTCTATTGTGTAACGC-3'. In Figure S7, *ptk7* riboprobe was synthesized from a 2068-bp fragment using the primers 5'-CGACTGTTAGTTGGTTTATGGAC-3', 5'-ACTTGCCTTCTCTTTGAGCG-3'. SMU15014980 and SMU15007112 (Robb et al. 2015) (<http://smedgd.stowers.org>) expression patterns were identified by in situ hybridization screening from genes defined as BPKG22168 and BPKG1900 by prior RNA-seq studies (Labbé et al. 2012). SMU15014980 was cloned using the primers 5'-GGATGCTTTTGCATTTTGCT -3' and 5'-ATTGGCAAGAAAGCCATGAG -3'. SMU15007112 was cloned using the primers 5'-CCCCGTGTGGATATTTCAAGT -3', 5'-AGCAAAATCGGTTCTCCGTA -3'. For inhibition of *ptk7*, dsRNA was synthesized from a 1412-bp cDNA fragment cloned by RT-PCR into pGEM vector using the primers 5'-TGCTGGAAATAGTCTGTTGCAT-3', 5'-AAGATGGAACCCCAATAGCC-3'. Control dsRNA was generated from a 1527-bp fragment of *Photinus pyralis luciferase* from the pGL3-control vector (Promega) (primers 5'-TATCCGCTGGAAGATGGAAC-3', 5'-CGGTACTTCGTCCACAAACA-3'). *wntP-2*

(Petersen and Reddien 2009), *ndl-3* (Rink et al. 2009), *laminin* (Adler et al. 2014), *porcupine* (Rink et al. 2009), *dmd-1*, *FoxA* (Adler et al. 2014), *smedwi-1*, *ndk*, *wnt1* (Petersen and Reddien 2009), *collagen* (Witchley et al. 2013), *chat*, *mag-1*, *cintillo*, *β -catenin-1* (Petersen and Reddien 2008), *APC* (Gurley et al. 2008), *wnt11-1* (Petersen and Reddien 2008), *wnt11-2* (Petersen and Reddien 2008), *wnt11-4/wntP-3* (Petersen and Reddien 2008), *wnt2* (Petersen and Reddien 2008), *wnt5* (Gurley et al. 2010), *fzd4-1* (Petersen and Reddien 2008), *fzd4-2*, *fzd-1/2/7*, *Dvl-1* (Gurley et al. 2008), *Dvl-2* (Gurley et al. 2008), *axin-B*, *teashirt* (Owen et al. 2015), *notum* (Petersen and Reddien 2011), *sfrp-1* (Gurley et al. 2010), *sfrp-2* (Gurley et al. 2010), *sfrp-3* (Gurley et al. 2010), *DAAMI* (Beane et al. 2012), *ROCK* (Beane et al. 2012), *vangl1*, *vangl2* (Almuedo-Castillo et al. 2011; Beane et al. 2012), and *ndl-4* (Rink et al. 2009) riboprobes and dsRNAs were described previously .

Fixations, whole-mount in situ hybridizations, and Concanavalin A staining

Animals were fixed and stained as previously described (Pearson et al. 2009; King and Newmark 2013). In brief, animals were killed in 5% N-acetyl-cysteine in 1xPBS for 5 minutes and then fixed in formaldehyde for 20 minutes at room temperature. Subsequently, animals were bleached overnight (~16 hours) in 6% hydrogen peroxide in methanol on a light box. Digoxigenin- or fluorescein-labeled riboprobes were synthesized as described previously (Pearson et al. 2009). Colorimetric (NBT/BCIP) or fluorescence in situ hybridizations were performed as previously described (Pearson et al. 2009; King and Newmark 2013). For FISH, blocking solution was MABT with 10% horse serum and 10% western blot blocking reagent (Roche) (King and Newmark 2013). Riboprobes were detected using anti-Dig-HRP (1:2000), anti-FL-HRP (1:2000), anti-DNP (1:2000), or anti-Dig-AP (1:4000) antibodies. Hoechst 33342 (Invitrogen) was used at 1:500 as counterstain. Images of colorimetric staining were acquired using a Leica M210F scope with a Leica DFC295 camera and adjusted for brightness and contrast. Fluorescence imaging was performed on a Leica DM5500B compound microscope with Optigrid structured illumination system for optical sectioning or a Leica SPE confocal microscope. Images are maximum projections of a z-series with adjustments to brightness and contrast using Photoshop or ImageJ. Concanavalin A conjugated to AlexaFluor 488 (Invitrogen) was used to stain the epidermis as described (Zayas et al. 2010).

Image analysis

For Figure 4B, animals stained with NBT/BCIP for detection of *ptk7*, *wntP-2*, and *ndl-3* were visualized with a Leica M210F dissecting microscope. Images were inverted and an intensity profile obtained from a segmented line drawn along a lateral region running from the anterior to posterior of the animal with a width approximately 1/6 of the animal width using ImageJ (“plot profile”). To make comparisons of intensity plots across animals of different sizes, position along the segmented line was normalized to its length. Background, taken as the minimum intensity along this profile, was subtracted, and the resulting values were normalized to the maximum intensity along this profile. This axis was divided into 100 equal sized bins to allow comparing intensity measurements across animals of different sizes, and the average normalized intensity was determined for each bin. These plots were compared for 4-6 animals stained with each riboprobe to generate an average and standard deviation of position- and global intensity-normalized in situ hybridization signal and plotted in Figure 4B.

In Figure 4C, Triple FISH was used to simultaneously detect expression of *ptk7*, *wntP-2*, and *ndl-3* by obtaining maximum projections of 1-micron thick confocal images taken at 40x at 8 regions. The resulting three-color images were processed in ImageJ to convert to a merged grayscale image used for automated thresholding (“Auto Threshold” Li's Minimum Cross Entropy method (Li 1998)) and segmentation (“Analyze particles”) using empirically optimized parameters (size=0.06-0.40 inch² in the image, corresponding to 24-166 microns² in the sample, and circularity 0-1.00). The resulting segmented areas were manually inspected to verify that the majority surrounded individual cells. Mean intensity per segmented area was determined for each channel and plotted using R (ggplot2) in Figure 4D and Figure 4E. In Figure 4 figure supplement 1A, density histograms were plotted to determine a cutoff for estimating high and low expression of each gene within each analyzed cell and used to classify cells as expression positive or negative. This assigned each cell to one of 8 classes plotted as a fraction of total cells in each region in a histogram in Figure 4 figure supplement 1B and as a scatterplot in Figure 4 figure supplement 1C. Similar trends were observed when threshold was taken to be any of 10 different threshold values between intensities of 30 and 75.

RNAi protocols

RNAi treatments were performed either by dsRNA injection or feeding. dsRNA was synthesized as described previously (Petersen and Reddien 2011). Unless otherwise noted, RNAi by injection was performed using a Drummond microinjector to deliver 5 x 32 nL dsRNA on three consecutive days, followed by transverse amputations and regeneration for the indicated number of days (Figures 1D,1E, 1S2, 2D,E, 3A,D, 3S1A,B, 5S1, 5S2, 5S3, 6A-D, 6S1, 6S2A, 6S4). For experiments involving RNAi by feeding, animals were given a mixture of liver paste and in vitro transcribed dsRNA, as described (Rouhana et al. 2013). In brief, animals were fed every 2-3 days for either 1 week (Figures 2S1, 5, 5S4, 6E, 6F) or 2 weeks (Figures 2A, 6S3) and were maintained homeostatically or allowed to regenerate for the indicated number of days prior to fixation. For long-term RNAi treatment in the absence of injury, animals were fed a mixture of liver paste and dsRNA every 2-3 days for 2 weeks, followed by one dsRNA feeding every subsequent week (Figure 2F). For RNAi treatment in sexual *S. mediterranea*, animals were fed dsRNA every 2-3 days for one week and amputated transversely to create trunk fragments containing the pharynx and reproductive structures including the copulatory apparatus then fed dsRNA once per week for 62 days (Figure 3S1C). For timed dsRNA delivery experiments (Figure 6S2B), RNAi-treated animals on days -2, -1, 0 were injected with dsRNA on three consecutive days, amputated transversely to create tail fragments on day 0, and animals fixed on day 7 of regeneration. For subsequent timed delivery of dsRNA, animals were amputated transversely to create tail fragments on day 0, followed by dsRNA injection for two consecutive days as indicated, and fixed on day 7 of regeneration.

Chemical amputation of pharynx in RNAi-treated animals

Animals were fed an equal mixture of *ptk7* and *wntP-2* dsRNA every 2-3 days for one week, amputated to remove heads and tails and allowed to regenerate for 20 days to produce an ectopic pharynx, then both the pre-existing and ectopic pharynges were removed by treatment with 100mM sodium azide as described previously (Adler et al. 2014). Animals were then fixed either 2 days or 19 days later and stained with *laminin* and *porcupine* riboprobes to assess regeneration of the ectopic pharynx (Figure 3C).

qPCR

Total RNA was extracted by mechanical homogenization in Trizol (Invitrogen) from three RNAi-treated intact animals, and purified in three biological replicates for each treatment. RNA samples were DNase-treated (TURBO DNase, Ambion) and cDNA was synthesized using SuperScript III reverse transcriptase (Invitrogen). qPCR was performed using SYBR Green PCR Master Mix (Applied Biosystems). *axin-B* mRNA was detected using the primers 5'-TTCCAGTTCAGGTCACATCG-3' and 5'-CATTGACACCTTCCGAACCT-3', *ubiquilin* mRNA was detected using 5'-AAATTCGCCTGCCTGTTGGG-3' and 5'-CCGGTGGCATTAATCCATCTGT-3', *clathrin* was detected using 5'-GACTGCGGGCTTCTATTGAG-3' and 5'-GCGGCAATTCTTCTGAACTC-3', *wntP-2* was detected using 5'-TGCTAAATCAACACCAGAATCAGCT-3' and 5'-CACATCCACAATTACTATGCACCCC-3', *ndl-3* was detected using 5'-CTCCCACAATTTATGAGTGCGGT-3' and 5'-TCTTGGGCCAATTTTGAGTTTTGATCTA-3', and *ptk7* was detected using 5'-GATCAAATCCCAAATCCAGTTC-3' and 5'-GGGTTTCTGGGAGTTTATATCGTA-3'. Relative RNA abundance was calculated using the delta-Ct method after verification of primer amplification efficiency. p-values were computed from a 2-tailed t-test.

References

- Adler CE, Sánchez Alvarado A (2015). Types or States? Cellular Dynamics and Regenerative Potential. *Trends Cell Biol.* 10.1016/j.tcb.2015.07.008
- Adler CE, Seidel CW, McKinney SA, Sánchez Alvarado A (2014) Selective amputation of the pharynx identifies a FoxA-dependent regeneration program in planaria. *eLife.* pp. e02238.
- Almuedo-Castillo M, Salo E, Adell T (2011). Dishevelled is essential for neural connectivity and planar cell polarity in planarians. *Proc Natl Acad Sci U S A* 108: 2813-2818. 10.1073/pnas.1012090108
- Beane WS, Tseng A, Morokuma J, Lemire J, Levin M (2012) Inhibition of Planar Cell Polarity Extends Neural Growth During Regeneration, Homeostasis and Development. *Stem Cells Dev.*
- Bin-Nun N, Lichtig H, Malyarova A, Levy M, Elias S, et al. (2014). PTK7 modulates Wnt signaling activity via LRP6. *Development* 141: 410-421. 10.1242/dev.095984
- Blassberg RA, Felix DA, Tejada-Romero B, Aboobaker AA (2013) PBX/extradenticle is required to re-establish axial structures and polarity during planarian regeneration. *Development.*
- Cebrià F, Kobayashi C, Umesono Y, Nakazawa M, Mineta K, et al. (2002) FGFR-related gene *nou-darake* restricts brain tissues to the head region of planarians. *Nature.* pp. 620-624.
- Chen CCG, Wang IE, Reddien PW (2013) *pbx* is required for pole and eye regeneration in planarians. *Development.*
- Chong T, Collins JJ, 3rd, Brubacher JL, Zarkower D, Newmark PA (2013). A sex-specific transcription factor controls male identity in a simultaneous hermaphrodite. *Nat Commun* 4: 1814. 10.1038/ncomms2811
- Currie KW, Pearson BJ (2013) Transcription factors *lhx1/5-1* and *pitx* are required for the maintenance and regeneration of serotonergic neurons in planarians. *Development.* pp. 3577-3588.
- Felix DA, Aboobaker AA (2010) The TALE Class Homeobox Gene *Smed-prep* Defines the Anterior Compartment for Head Regeneration. *PLoS Genet.* pp. e1000915.

- 927 Fraguas S, Barberan S, Iglesias M, Rodriguez-Esteban G, Cebria F (2014) egr-4, a target of
928 EGFR signaling, is required for the formation of the brain primordia and head
929 regeneration in planarians. *Development*. pp. 1835-1847.
- 930 French V, Bryant PJ, Bryant SV (1976). Pattern regulation in epimorphic fields. *Science* 193:
931 969-981.
- 932 Gerber SD, Steinberg F, Beyeler M, Villiger PM, Trueb B (2009). The murine Fgfr11 receptor is
933 essential for the development of the metanephric kidney. *Dev Biol* 335: 106-119.
934 10.1016/j.ydbio.2009.08.019
- 935 Gurley KA, Elliott SA, Simakov O, Schmidt HA, Holstein TW, et al. (2010) Expression of
936 secreted Wnt pathway components reveals unexpected complexity of the planarian
937 amputation response. *Dev Biol: Elsevier Inc.* pp. 24-39.
- 938 Gurley KA, Rink JC, Sánchez Alvarado A (2008) Beta-Catenin Defines Head Versus Tail
939 Identity During Planarian Regeneration and Homeostasis. *Science*. pp. 323-327.
- 940 Hayes M, Naito M, Daulat A, Angers S, Ciruna B (2013). Ptk7 promotes non-canonical
941 Wnt/PCP-mediated morphogenesis and inhibits Wnt/beta-catenin-dependent cell fate
942 decisions during vertebrate development. *Development* 140: 1807-1818.
943 10.1242/dev.090183
- 944 Iglesias M, Gomez-Skarmeta JL, Saló E, Adell T (2008) Silencing of Smed- β catenin1 generates
945 radial-like hypercephalized planarians. *Development*. pp. 1215-1221.
- 946 King RS, Newmark PA (2013) In situ hybridization protocol for enhanced detection of gene
947 expression in the planarian *Schmidtea mediterranea*. *BMC Dev Biol*. pp. 8.
- 948 Kobayashi C, Saito Y, Ogawa K, Agata K (2007) Wnt signaling is required for antero-posterior
949 patterning of the planarian brain. *Dev Biol*. pp. 714-724.
- 950 Labbé RM, Irimia M, Currie KW, Lin A, Zhu SJ, et al. (2012) A Comparative Transcriptomic
951 Analysis Reveals Conserved Features of Stem Cell Pluripotency in Planarians and
952 Mammals. *Stem Cells*. pp. 1734-1745.
- 953 Lhoumeau AC, Puppo F, Prebet T, Kodjabachian L, Borg JP (2011). PTK7: a cell polarity
954 receptor with multiple facets. *Cell Cycle* 10: 1233-1236.
- 955 Li CaT, PKS (1998). An Iterative Algorithm for Minimum Cross Entropy Thresholding. *Pattern*
956 *Recognition Letters* 18: 5.

957 Lu X, Borchers AG, Jolicoeur C, Rayburn H, Baker JC, et al. (2004). PTK7/CCK-4 is a novel
958 regulator of planar cell polarity in vertebrates. *Nature* 430: 93-98. 10.1038/nature02677

959 Marz M, Seebeck F, Bartscherer K (2013) A Pitx transcription factor controls the establishment
960 and maintenance of the serotonergic lineage in planarians. *Development*. pp. 4499-4509.

961 Oviedo NJ, Morokuma J, Walentek P, Kema IP, Gu MB, et al. (2010) Long-range neural and gap
962 junction protein-mediated cues control polarity during planarian regeneration. *Dev Biol*.
963 pp. 188-199.

964 Owen JH, Wagner DE, Chen CC, Petersen CP, Reddien PW (2015). teashirt is required for head-
965 versus-tail regeneration polarity in planarians. *Development* 142: 1062-1072.
966 10.1242/dev.119685

967 Pearson BJ, Eisenhoffer GT, Gurley KA, Rink JC, Miller DE, et al. (2009) Formaldehyde-based
968 whole-mount in situ hybridization method for planarians. *Dev Dyn*. pp. 443-450.

969 Peradziryi H, Kaplan NA, Podleschny M, Liu X, Wehner P, et al. (2011). PTK7/Otk interacts
970 with Wnts and inhibits canonical Wnt signalling. *EMBO J* 30: 3729-3740.
971 10.1038/emboj.2011.236

972 Petersen CP, Reddien PW (2008) Smed- β catenin-1 Is Required for Anteroposterior Blastema
973 Polarity in Planarian Regeneration. *Science*. pp. 327-330.

974 Petersen CP, Reddien PW (2009) Wnt Signaling and the Polarity of the Primary Body Axis. *Cell*.
975 pp. 1056-1068.

976 Petersen CP, Reddien PW (2009) A wound-induced Wnt expression program controls planarian
977 regeneration polarity. *Proc Natl Acad Sci USA*. pp. 17061-17066.

978 Petersen CP, Reddien PW (2011) Polarized notum Activation at Wounds Inhibits Wnt Function
979 to Promote Planarian Head Regeneration. *Science*. pp. 852-855.

980 Puppo F, Thome V, Lhoumeau AC, Cibois M, Gangar A, et al. (2011). Protein tyrosine kinase 7
981 has a conserved role in Wnt/beta-catenin canonical signalling. *EMBO Rep* 12: 43-49.
982 10.1038/embor.2010.185

983 Reddien PW (2011) Constitutive gene expression and the specification of tissue identity in adult
984 planarian biology. *Trends Genet: Elsevier Ltd*. pp. 277-285.

985 Reuter H, Marz M, Vogg MC, Eccles D, Grifol-Boldu L, et al. (2015). Beta-catenin-dependent
986 control of positional information along the AP body axis in planarians involves a teashirt
987 family member. *Cell Rep* 10: 253-265. 10.1016/j.celrep.2014.12.018

988 Riddiford N, Olson PD (2011). Wnt gene loss in flatworms. *Dev Genes Evol* 221: 187-197.
989 10.1007/s00427-011-0370-8

990 Rink JC, Gurley KA, Elliott SA, Sánchez Alvarado A (2009) Planarian Hh Signaling Regulates
991 Regeneration Polarity and Links Hh Pathway Evolution to Cilia. *Science*. pp. 1406-1410.

992 Robb SM, Gotting K, Ross E, Sanchez Alvarado A (2015). SmedGD 2.0: The Schmidtea
993 mediterranea genome database. *Genesis* 53: 535-546. 10.1002/dvg.22872

994 Roensch K, Tazaki A, Chara O, Tanaka EM (2013). Progressive specification rather than
995 intercalation of segments during limb regeneration. *Science* 342: 1375-1379.
996 10.1126/science.1241796

997 Rouhana L, Weiss JA, Forsthoefel DJ, Lee H, King RS, et al. (2013) RNA interference by
998 feeding in vitro-synthesized double-stranded RNA to planarians: methodology and
999 dynamics. *Dev Dyn*. pp. 718-730.

1000 Scimone ML, Lapan SW, Reddien PW (2014) A forkhead Transcription Factor Is Wound-
1001 Induced at the Planarian Midline and Required for Anterior Pole Regeneration. *PLoS*
1002 *Genet*. pp. e1003999.

1003 Stark K, Vainio S, Vassileva G, McMahon AP (1994). Epithelial transformation of metanephric
1004 mesenchyme in the developing kidney regulated by Wnt-4. *Nature* 372: 679-683.
1005 10.1038/372679a0

1006 Tejada-Romero B, Carter JM, Mihaylova Y, Neumann B, Aboobaker AA (2015). JNK signalling
1007 is necessary for a Wnt- and stem cell-dependent regeneration programme. *Development*
1008 142: 2413-2424. 10.1242/dev.115139

1009 Vásquez-Doorman C, Petersen CP (2014) zic-1 Expression in Planarian Neoblasts after Injury
1010 Controls Anterior Pole Regeneration. *PLoS Genet*. pp. e1004452.

1011 Vogg MC, Owlarn S, Pérez Rico YA, Xie J, Suzuki Y, et al. (2014) Stem cell-dependent
1012 formation of a functional anterior regeneration pole in planarians requires Zic and
1013 Forkhead transcription factors. *Dev Biol*. pp. 136-148.

1014 Witchley JN, Mayer M, Wagner DE, Owen JH, Reddien PW (2013) Muscle Cells Provide
1015 Instructions for Planarian Regeneration. *Cell Reports: The Authors*. pp. 633-641.

1016 Wolpert L (1969). Positional information and the spatial pattern of cellular differentiation. *J*
1017 *Theor Biol* 25: 1-47.

- 1018 Zayas RM, Cebria F, Guo T, Feng J, Newmark PA (2010). The use of lectins as markers for
1019 differentiated secretory cells in planarians. Dev Dyn 239: 2888-2897.
1020 10.1002/dvdy.22427
- 1021 Zhang D, Chan JD, Nogi T, Marchant JS (2011) Opposing Roles of Voltage-Gated Ca²⁺
1022 Channels in Neuronal Control of Regenerative Patterning. J Neurosci. pp. 15983-15995.
1023

Figure 1

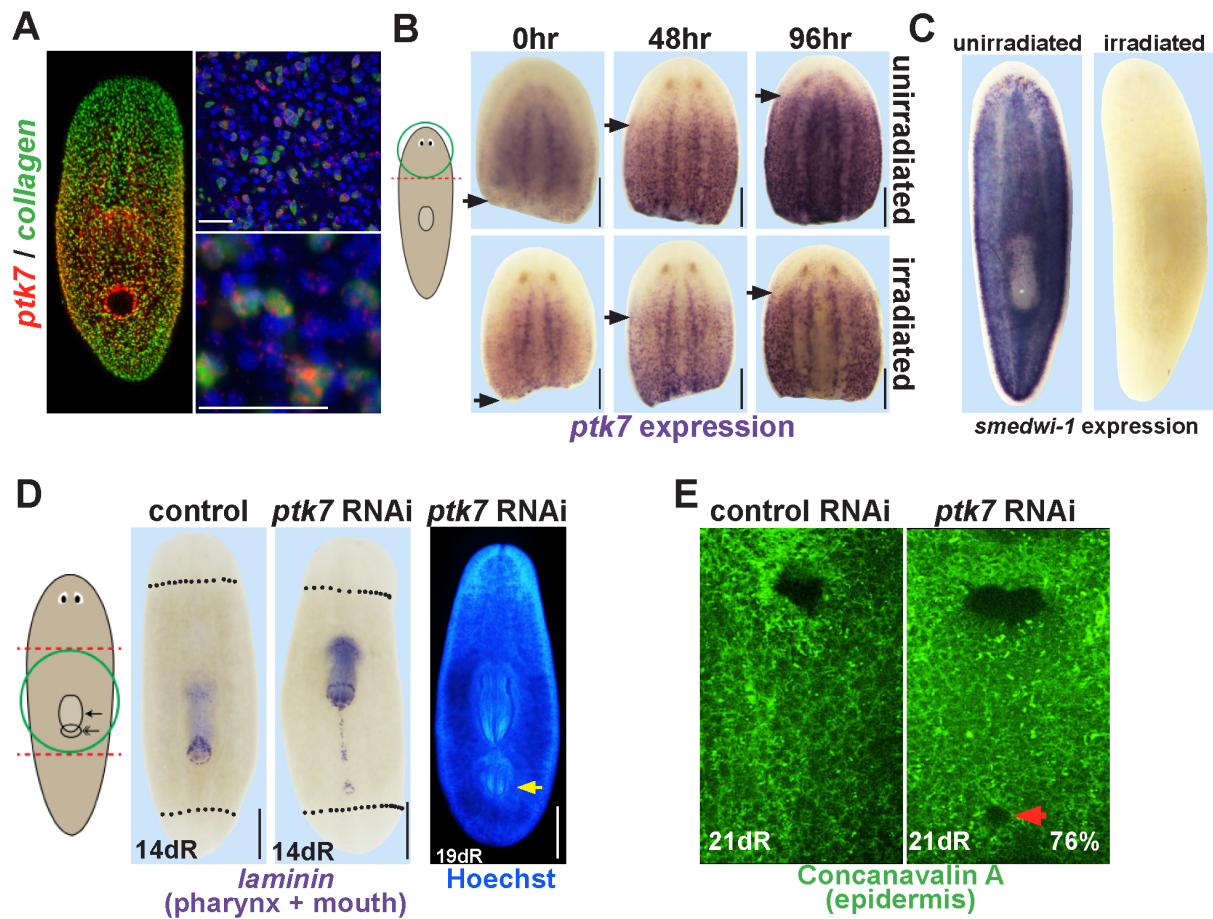
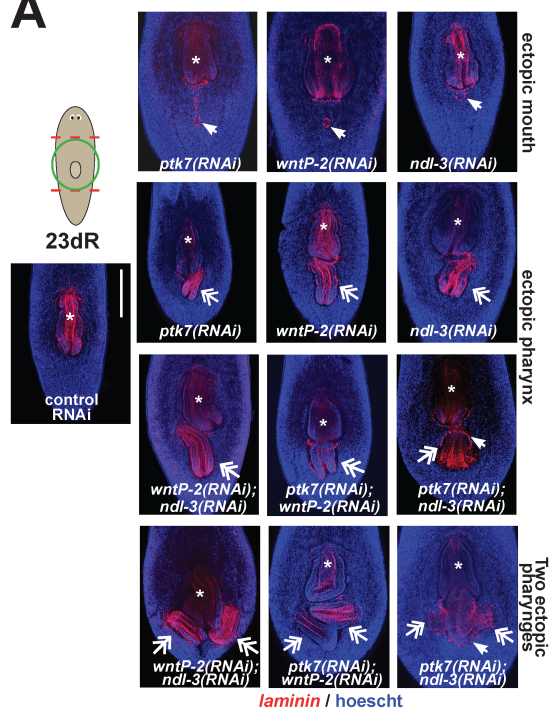
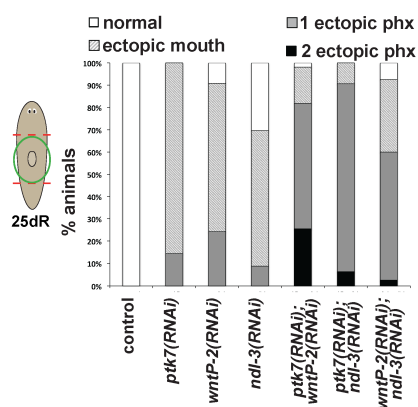


Figure 2

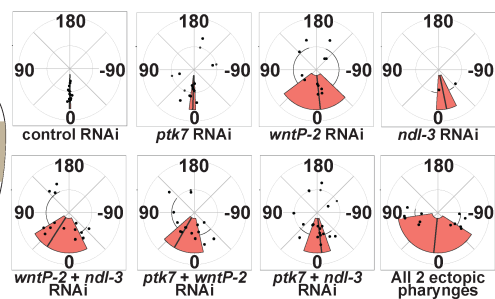
A



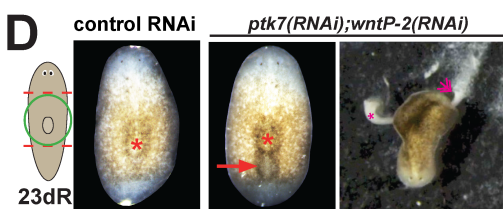
B



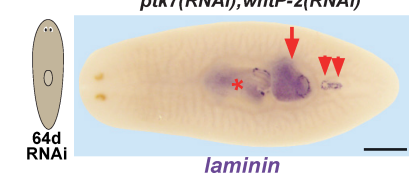
C



D



E



F

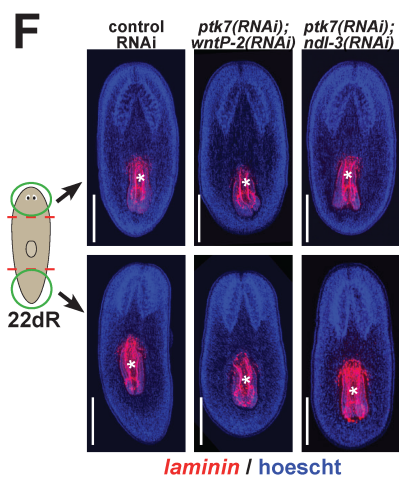


Figure 3

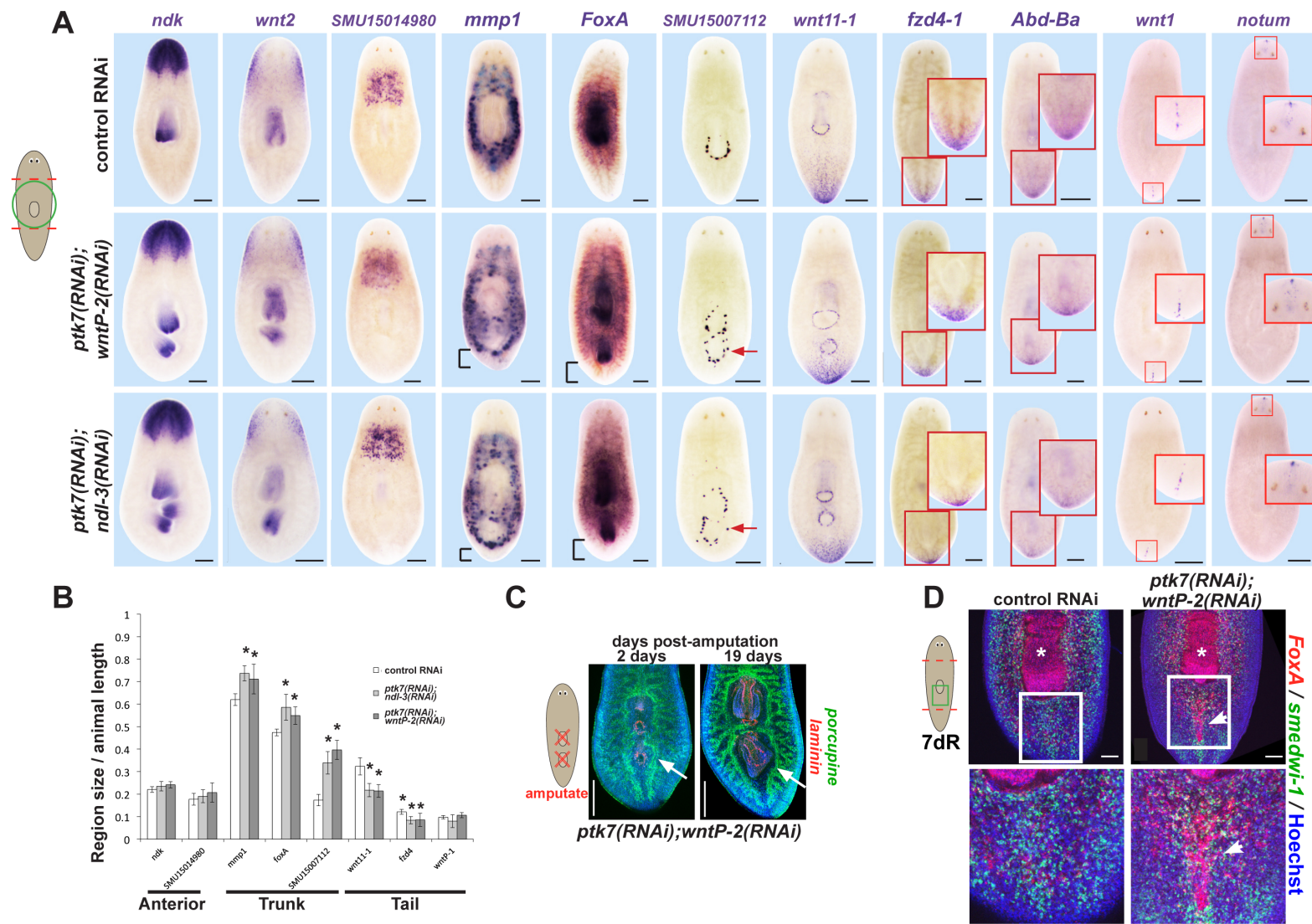


Figure 4

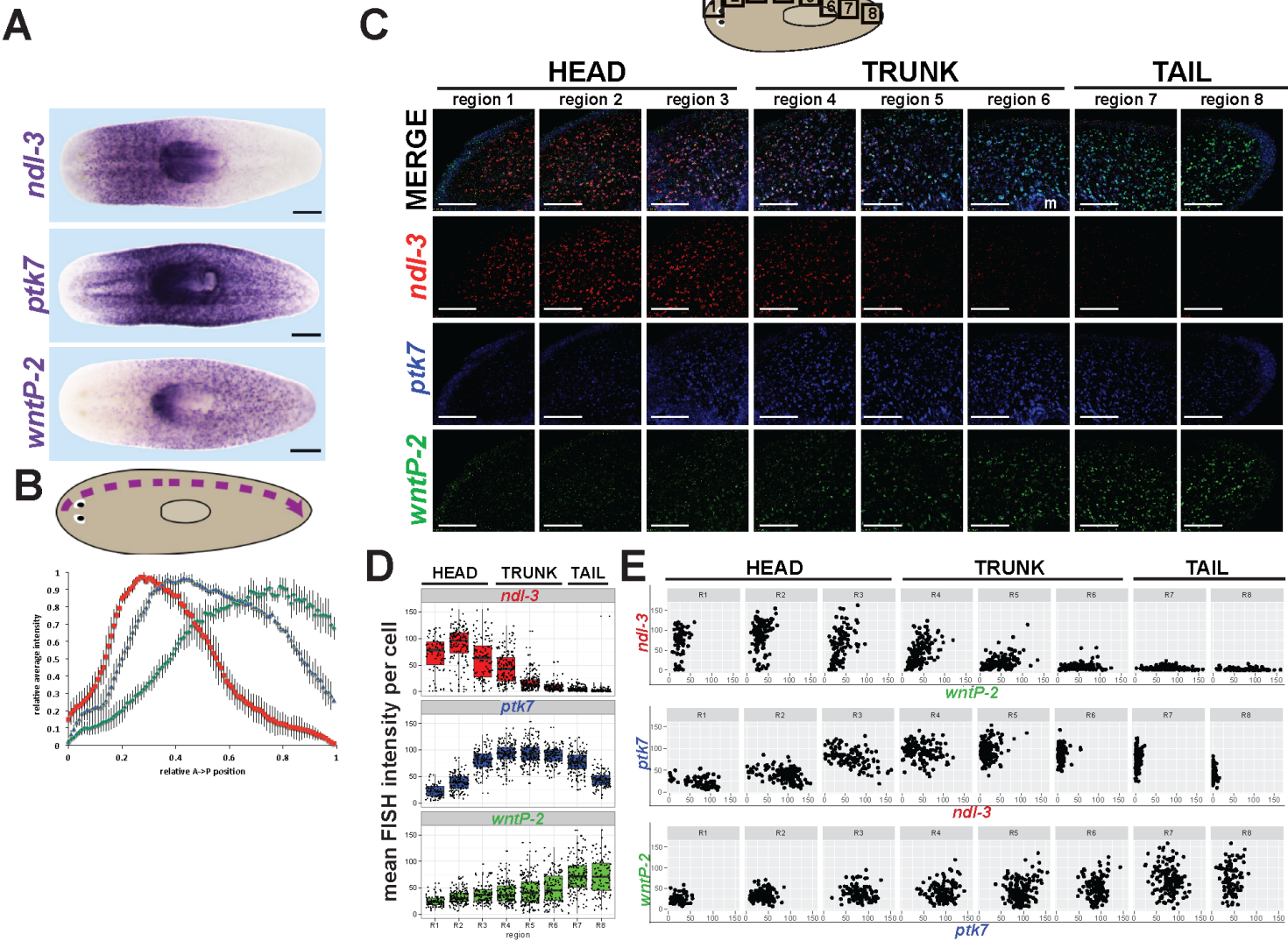


Figure 5

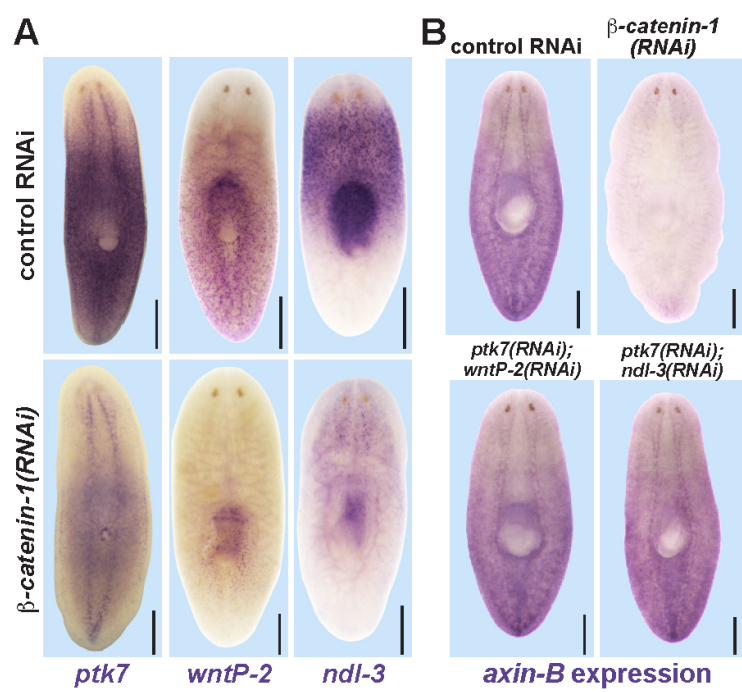


Figure 6

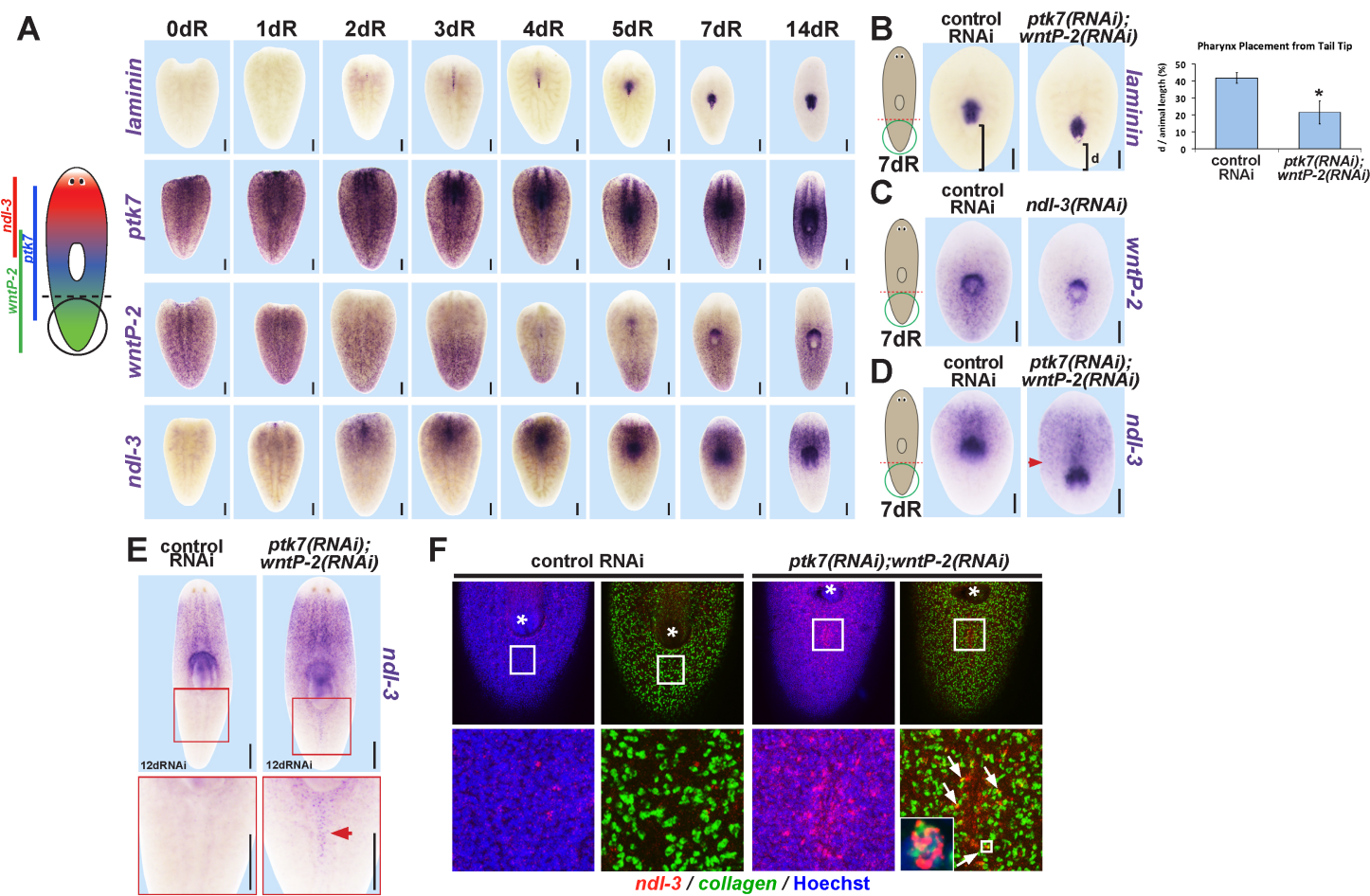


Figure 7

